

# On the Validity of Constant pH Simulations

Amin Bakhshandeh and Yan Levin\*



Cite This: *J. Chem. Theory Comput.* 2024, 20, 1889–1896



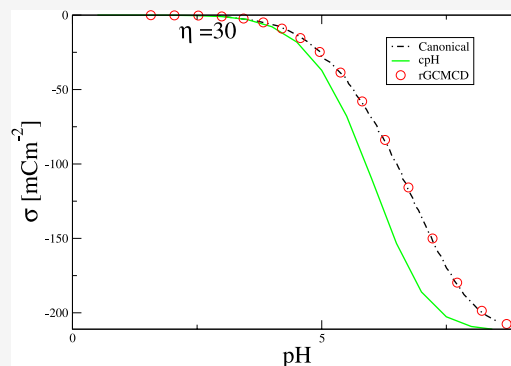
Read Online

ACCESS |

Metrics & More

Article Recommendations

**ABSTRACT:** Constant pH (cpH) simulations are now a standard tool for investigating charge regulation in coarse-grained models of polyelectrolytes and colloidal systems. Originally developed for studying solutions with implicit ions, extending this method to systems with explicit ions or solvents presents several challenges. Ensuring proper charge neutrality within the simulation cell requires performing titration moves in sync with the insertion or deletion of ions, a crucial aspect often overlooked in the literature. Contrary to the prevailing views, cpH simulations are inherently grand-canonical, meaning that the controlled pH is that of the reservoir. The presence of the Donnan potential between the implicit reservoir and the simulation cell introduces significant differences between titration curves calculated for open and closed systems; the pH of an isolated (closed) system is different from the pH of the reservoir for the same protonation state of the polyelectrolyte. To underscore this point, in this paper, we will compare the titration curves calculated using the usual cpH algorithm with those from the exact canonical simulation algorithm. In the latter case, titration moves adhere to the correct detailed balance condition, and pH is calculated using the recently introduced surface Widom insertion algorithm. Our findings reveal a very significant difference between the titration isotherms obtained using the standard cpH algorithm and the canonical titration algorithm, emphasizing the importance of using the correct simulation approach when studying charge regulation of polyelectrolytes, proteins, and colloidal particles.



## INTRODUCTION

The effective charge of colloidal particles and polymers, produced by weak acid or weak base functional groups, experiences variation with environmental pH due to the ionization of these groups.<sup>1–14</sup> The  $\text{pH} = -\log_{10}(a_{\text{H}})$ <sup>15</sup> is defined as the negative decadic logarithm of dimensionless proton activity,  $a_{\text{H}} = c_{\text{H}}e^{\beta\mu_{\text{H}}^{\text{ex}}}/c^{\ominus}$ , where  $c^{\ominus} = 1 \text{ M}$  is the standard concentration and  $\beta = 1/k_{\text{B}}T$  and  $\mu_{\text{H}}^{\text{ex}}$  denotes the excess electrochemical potential.<sup>16</sup>

The stability of colloidal particles in aqueous suspensions is intrinsically connected with their surface charge density, which is controlled by the pH of the solution. Similarly, the activity of many biologically relevant proteins and polyelectrolytes is influenced by the solution's pH and ionic strength.<sup>6,8,16–33</sup> A quantitative understanding of charge regulation in such complex systems is therefore crucial for a wide range of industrial and medical applications.

For some simple colloidal systems, one can use the Poisson–Boltzmann theory with the charge regulation boundary condition to study the degree of protonation.<sup>1,2,10–14,34–40</sup> However, this approach breaks down for suspensions containing salts with multivalent counterions or when studying flexible molecules—such as proteins, polyelectrolytes, polyampholytes, etc., whose three-dimensional conformation is directly determined by the protonation state of the macromolecules. To overcome this difficulty, in 1992, Reed

& Reed (RR) proposed a constant pH (cpH) Monte Carlo (MC) simulation method,<sup>3,41</sup> to calculate the titration curves for such systems. Originally, the RR-cpH algorithm was applied to systems with implicit ions—the monomers interact with each other through the screened Coulomb potential—soon after, however, extensions to systems with explicit ions were proposed.<sup>3</sup> To preserve the overall charge neutrality in such approaches, a protonation move is combined with an arbitrary deletion of one hydronium ion inside the cell, and a deprotonation move with an arbitrary insertion of a hydronium ion at a random position inside the cell. Such arbitrary insertion/deletion of ions inside the simulation cell, however, violates the detailed balance condition, leading to incorrect results.<sup>42–44</sup> The problem with the RR-cpH algorithm, when applied to explicit ions, was pointed out some 20 years ago by Labbez and Jönsson,<sup>42</sup> but unfortunately went unnoticed inside the physical chemistry and soft matter communities, where RR-cpH became very popular to treat various systems in which charge regulation plays an important role.<sup>3</sup> An

Received: December 12, 2023

Revised: January 29, 2024

Accepted: February 1, 2024

Published: February 15, 2024



alternative canonical approach to calculating the titration curves was proposed by Ullner and Woodward. These authors used a closed spherical simulation cell with a fixed number of protons. They then used the Widom insertion method to obtain the chemical potential inside the system for a given protonation state.<sup>45</sup>

Contrary to a common misconception, the RR-cpH algorithm is not a canonical algorithm.<sup>46</sup> For isolated systems, the total number of protons is conserved, and the titration algorithm must use the correct canonical acceptance probabilities for the protonation/deprotonation moves, which do not explicitly depend on the pH inside the simulation cell.<sup>43,47–49</sup> In a canonical (isolated) system, pH is not a control parameter—it cannot be specified a priori, but can only be calculated *a posteriori*, after the simulation has fully equilibrated, and the number of protonated groups has been determined.<sup>49</sup> Therefore, if one wants to modify the RR-cpH algorithm to properly include the explicit ions, one must take into account that the simulation cell is implicitly in contact with an external reservoir of acid and salt.<sup>43,50</sup> A protonation/deprotonation move should then be combined with the simultaneous insertion/deletion of an anion from the reservoir, in accordance with the correct grand canonical (GC) acceptance probability.<sup>42,43,50</sup> Furthermore, since in such a simulation polyelectrolyte is confined within the cell, while ions can freely exchange between the system and the reservoir, the two will be at different electrostatic potentials.<sup>44,50</sup> This is known as the “Donnan potential”,  $\varphi_D$ . The presence of the Donnan potential between the implicit reservoir and the simulation cell introduces a significant difference between the titration curves calculated for open and closed systems—the  $\text{pH}_c$  of an isolated (closed) system is different from the  $\text{pH}_R$  of the reservoir, for the same protonation state of the polyelectrolyte.<sup>43,44,51</sup> When discussing the pH of inhomogeneous systems, such as a polyelectrolyte solution separated from the reservoir of acid and salt by a semipermeable membrane, it is usual to define activity by separating the mean-electrostatic potential within the phase. Such a definition is equivalent to placing the reference (saturated calomel) and hydrogen electrodes within the same phase when measuring the pH.<sup>51</sup> The equivalence of the electrochemical potential of hydronium ions across the membrane is then expressed as  $\ln a_{\text{H}^+}^{\text{S}} + \beta q \varphi_D = \ln a_{\text{H}^+}^{\text{R}}$ , where  $a_{\text{H}^+}^{\text{S}}$  is the activity of hydronium ions inside the polyelectrolyte solution (system) and  $a_{\text{H}^+}^{\text{R}}$  is the activity inside the reservoir. The pH inside the system is then defined as  $\text{pH}_S = -\log_{10}(a_{\text{H}^+}^{\text{S}})$  and inside the reservoir as  $\text{pH}_R = -\log_{10}(a_{\text{H}^+}^{\text{R}})$ . In a recent paper, we have discussed the problems that may arise due to the violation of the Gibbs-Guggenheim principle,<sup>51</sup> when mean-electrostatic potential is excluded from the definition of activity. Nevertheless, since this is the usual convention, we will adopt it in the present paper. The pH inside the system is then different from that of the reservoir.<sup>45</sup> Furthermore, if, after the equilibrium is established, the system is disconnected from the reservoir (is closed), its  $\text{pH}_S$  will not be affected. Therefore, if we would perform a canonical reactive simulation on such a closed system, we will obtain exactly the same pH, i.e.,  $\text{pH}_c = \text{pH}_S$ . The relation between pH inside the system and pH in the reservoir is then<sup>44</sup>

$$\text{pH}_S = \text{pH}_R + \frac{q\beta\varphi_D}{\ln(10)} \quad (1)$$

This allows us to use GC simulations, in which the chemical potential of hydronium ions ( $\text{pH}_R$ ) is specified inside the reservoir, to determine the  $\text{pH}_c = \text{pH}_S$  inside an isolated system. To do this, however, requires knowledge of the Donnan potential difference between the system and the reservoir.

To preserve charge neutrality, usual GC simulation methods involve the insertion of neutral pairs of ions into the system, making the Donnan potential cancel in the acceptance probability of such pair moves. This prevents us from obtaining the Donnan potential using such approaches.<sup>50,52</sup> Therefore, a corrected cpH algorithm, in which the charge neutrality is properly taken into account through the pairwise insertions, will only allow us to calculate the protonation state of polyelectrolyte as a function of  $\text{pH}_R$  inside the reservoir and not the  $\text{pH}_S$  inside the system (simulation cell). On the other hand, most experiments are conducted on closed systems, which, according to 1 will have a different pH from that of the reservoir. Recently, we have developed a new reactive GC MC Donnan (rGCMCD) simulation method that allows us to calculate both the Donnan potential and the protonation state of polyelectrolyte solution in contact with a reservoir of acid and salt.<sup>44</sup> Equation 1 then permits us to simultaneously calculate the titration isotherms for an open system, as a function of pH in the reservoir; and for a closed system, as a function of pH inside the simulation cell.

If one is interested in studying closed systems, the rGCMCD approach is not very convenient since it calls for the specification of the chemical potential of all ions inside the reservoir in order to perform the GC moves. This requires a separate simulation of the reservoir, in which, the Widom insertion method is used to obtain the chemical potential of all the ions.<sup>53–57</sup> Furthermore, the calculation of the Donnan potential within the GC formalism makes such simulations slow. Recently, we have developed a new method for canonical titration simulations utilizing the surface Widom insertion algorithm that enables us to easily calculate equilibrium pH.<sup>49</sup> In such systems, the traditional Widom insertion method cannot be used since at high pH, there may be few or no hydronium ions present inside the simulation cell, preventing us from accurately determining the chemical potential of these ions. The difficulty of calculating pH in canonical reactive simulations is probably one of the reasons for the widespread use of the incorrect RR-cpH algorithm in the soft matter and biophysics literature.<sup>3</sup>

The primary objective of this paper is to quantitatively explore the limitations of the RR-cpH algorithm. To achieve this, we compare the RR-cpH algorithm with three different methods: the surface Widom canonical reactive simulation, the rGCMCD simulations, and the pair insertion simulations for systems with high salt content. At high ionic strength, the Donnan potential vanishes, and the titration isotherms for open and closed systems become identical. We will see that canonical, pair, and rGCMCD methods agree perfectly between themselves, while they disagree strongly from the RR-cpH algorithm, showing its complete failure under a very wide range of experimental conditions.

## ■ RR-CPH ALGORITHM

In this methodology, dissociation and association reactions of polyelectrolyte monomers occur with probabilities linked to the acid dissociation constant  $K_a$  of the reaction<sup>3</sup>



For the forward direction (deprotonation), a site of a polyelectrolyte undergoes a change from 0 to  $-q$ , where  $q$  is the proton charge, while simultaneously a hydronium ion is “created” at a random position inside the cell. Conversely, in the backward reaction (protonation move), a negatively charged site is neutralized and, simultaneously, one random hydronium ion is deleted from the cell. The simulation starts with a charge neutral system, so that for each negative site of polyelectrolyte, there is a hydronium ion present in the bulk of the cell.

The acceptance probabilities for forward and reverse reactions are<sup>3,43</sup>

$$P = \min[1, \exp(-\beta\Delta U + \zeta(\text{pH} - \text{p}K_a)\ln(10))] \quad (3)$$

where  $\Delta U$  is the change in electrostatic energy,  $\text{p}K_a = -\log_{10}(K_a/c^\ominus)$  and  $\zeta = \pm 1$  for deprotonation and protonation moves, respectively.

In the RR-cpH algorithm, one specifies the pH and concentrations of ions and the polyelectrolyte inside the simulation cell as the input parameters. The method then provides the degree of ionization along with ensemble averages of observables after equilibrium has been established. It is often stated that the pH in eq 3 corresponds to the pH inside the canonical simulation cell.<sup>46</sup> This, however, is not correct. In a canonical reactive MC simulation, the total number of protons inside the system is fixed, and the simulation algorithm then determines how many of these protons will remain free (in the form of hydronium ions) and how many will become associated with the polyelectrolyte surface groups. The pH of the system, which is related to the electrochemical potential of hydronium ions, does not make part of the detailed balance condition and cannot appear in the acceptance probabilities of titration moves. The correct canonical reactive MC algorithm is presented in the following section.

In order to understand the shortfalls of eq 3, it is crucial to first recognize that RR-cpH algorithm is inherently GC. This is evident when examining the weight for a protonation move in eq 3, in which appears  $e^{-\ln(10)\text{pH}} \sim e^{\beta\mu_{\text{H}}}$ , where  $\mu_{\text{H}}$  is the electrochemical potential of a hydronium ion. This is precisely the GC weight associated with transferring a hydronium ion from the reservoir to the simulation cell. In the context of the GCMC simulations of Coulomb systems, maintaining charge neutrality within the simulation cell is paramount, in particular, when using Ewald summation to treat long-range Coulomb interaction. Consequently, a GC protonation move necessitates a corresponding GC insertion move for an anion, and a deprotonation move should be coupled with a GCMC removal of an anion to preserve the overall charge neutrality inside the system. One cannot arbitrarily delete or create ions inside the simulation cell, as is usually done in the framework of the RR-cpH algorithm.<sup>3</sup> Instead, ions must be inserted or removed from the system with the correct GC acceptance probabilities.

## CANONICAL ENSEMBLE METHOD

Consider now a closed system containing polyions with titratable surface groups, salt and acid. We can start the system in an initial state in which all polyelectrolyte groups are completely deprotonated, with the corresponding number of hydronium ions placed in the bulk of the simulation cell. The cell also contains ions derived from the dissociation of salt, say  $\text{Na}^+$  and  $\text{Cl}^-$ . The reactive MC simulation then determines

how many of the polyelectrolyte groups will become protonated in equilibrium. The acceptance probabilities for deprotonation/protonation moves are given by<sup>43,47–49</sup>

$$P_{\text{d}} = \min\left[1, \frac{VN_{\text{A}}K_{\text{a}}}{N_{\text{H}} + 1} e^{-\beta\Delta U}\right]$$

$$P_{\text{p}} = \min\left[1, \frac{N_{\text{H}}}{VN_{\text{A}}K_{\text{a}}} e^{-\beta\Delta U}\right] \quad (4)$$

where  $N_{\text{H}}$  is the number of free hydronium ions inside the simulation cell at a given moment and  $N_{\text{A}}$  is the Avogadro number. Note that for canonical (closed) systems, the acceptance probabilities do not explicitly depend on pH. The pH of the system, after the equilibrium is established, has to be calculated using a separate procedure that require the determination of the chemical potential of hydronium ions inside the simulation cell. The conventional approach of employing Widom’s particle insertion method encounters practical challenges for moderate and high pH when a cell’s interior has few or maybe even no free hydroniums at all, resulting in a very inaccurate reading of the chemical potential of hydronium ions. To overcome this difficulty, we have recently introduced a surface Widom insertion algorithm, which allows us to easily calculate the pH inside the system after equilibrium has been established.<sup>49</sup>

One difficulty when working with Coulomb systems is that we cannot cutoff the long-range electrostatic interactions between particles and use simple periodic boundary conditions. Instead, the system has to be infinitely replicated. To efficiently sum the replicas, we use the Ewald summation method, which effectively creates a spherical macroscopic crystal composed of periodically replicated microscopic simulation cells.<sup>58–61</sup> Typically, a simulation cell will have a net electric dipole moment,  $\mathbf{M} = \sum_i q_i \mathbf{r}_i$ , and a finite second-moment tensor of the charge density. Electrostatically, the field produced by a dielectric sphere of uniform polarizability  $\mathbf{M}$  is equivalent to that of a sphere with nonuniform surface charge density  $\mathbf{M} \cdot \mathbf{n}/V$ , where  $\mathbf{n}$  represents the unit normal to the surface of the macroscopic sphere. The existence of an effective surface charge induces an electric field within the crystal’s interior. Simultaneously, the existence of a nonzero second-moment tensor of the charge density in the simulation cell results in a dipole layer at the macroscopic crystal’s surface.<sup>44,62</sup> This leads to a difference between the mean electrostatic potentials inside and outside the crystal. This potential difference is known as the Bethe potential<sup>49</sup>

$$\phi_{\text{B}} = -\frac{2\pi}{3\epsilon_{\text{w}}V} \sum_i q_i r_i^2 \quad (5)$$

where  $\epsilon_{\text{w}}$  is the dielectric constant of the medium (water). To quantitatively explore the difference between the titration isotherms calculated using the standard RR-cpH algorithm, eq 3, and the canonical algorithm, eq 4, we focus on a colloidal particle with  $Z$  active surface groups placed at the center of a cubic simulation cell of volume  $V = L^3$ , where  $L$  is the side length of the cell. The cell also contains  $\text{H}_3\text{O}^+$ ,  $\text{Cl}^-$ , and  $\text{Na}^+$  ions, ensuring overall charge neutrality. We execute the reactive MC simulation to ascertain the average number of protonated surface groups after equilibrium has been established. We then use the surface Widom insertion method to obtain the pH inside the system.<sup>49</sup> Briefly, the idea behind



the surface Widom method involves bringing a virtual proton from infinity to a randomly chosen colloidal active site. If the selected site is unoccupied (bearing charge  $-q$ ), it “reacts” with the virtual proton, causing its charge to transition to 0. We then calculate the change in the electrostatic energy between the initial and final states  $\Delta U$ . If the site is already occupied, then  $\Delta U$  is infinite. The system’s pH is then given by<sup>49</sup>

$$\text{pH} = -\log_{10}\left(\frac{N+1}{Z}\right) + \text{pK}_a + \log_{10}(\langle e^{-\beta(\Delta U + q\phi_b)} \rangle_0) \quad (6)$$

where  $N$  is the number of protonated sites at equilibrium. The average in eq 6 is calculated using 5000 uncorrelated virtual proton insertions, and the subscript 0 in the parentheses signifies that the evolution of the system between the virtual proton insertion events is performed with the unperturbed Hamiltonian.

The electrostatic energy inside the system is calculated using the Ewald formalism<sup>44</sup>

$$U = \frac{1}{2} \sum_{ij} \sum_n \frac{q_i q_j \text{erfc}(\kappa_e |r_i - r_j - L\mathbf{n}|)}{\epsilon_w |r_i - r_j - L\mathbf{n}|} + \sum_{\mathbf{k} \neq 0} \frac{2\pi \exp(-\mathbf{k}^2/4\kappa_e)}{\epsilon_w V \mathbf{k}^2} (A(\mathbf{k})^2 + B(\mathbf{k})^2) - \sum_i \frac{q_i^2 \kappa_e}{\epsilon_w \sqrt{\pi}} - \frac{Q_t^2}{2\epsilon_w V \kappa_e^2} + \frac{2\pi}{3\epsilon_w V} M^2 \quad (7)$$

where

$$A(\mathbf{k}) = \sum_i q_i \cos(\mathbf{k} \cdot \mathbf{r}_i), \\ B(\mathbf{k}) = \sum_i q_i \sin(\mathbf{k} \cdot \mathbf{r}_i) \quad (8)$$

In eq 7,  $\mathbf{n} = (n_1, n_2, n_3)$  is the integer vectors,  $\mathbf{k} = \left(\frac{2\pi}{L}n_1, \frac{2\pi}{L}n_2, \frac{2\pi}{L}n_3\right)$  is the reciprocal lattice vectors,  $Q_t = \sum_i q_i$  is the total charge inside the simulation cell, and  $\kappa_e$  is the damping parameter. The prime on the first sum of eq 7 signifies the exclusion of the terms  $i = j$  for  $\mathbf{n} = 0$ . In the calculation of  $U$ , we use the tin foil boundary condition<sup>49</sup> that eliminates the  $M^2$  term in eq 7. Note that if one places a virtual proton into the system, then it will no longer be charge neutral. A periodically replicated charge non-neutral system will have infinite energy. To avoid this in the calculation of eq 7, we have introduced a uniform neutralizing background.<sup>44</sup> In practice, to calculate Ewald sums, we used 600  $k$ -vectors. The damping parameter is set to  $\kappa_e = S/L$ , so that we can use simple periodic boundary conditions for calculating the short-range-erfc term in eq 7 contribution to the total electrostatic energy.

Titration is performed by adding NaOH base to the system. Since hydrolysis of water is so weak, the addition of one  $\text{OH}^-$  will result in a reaction with the hydronium ion inside the cell and the appearance of a new water molecule. Within the present implicit water model, the addition of one sodium hydroxide molecule is then equivalent to replacing one proton inside the simulation cell with a sodium ion,  $\text{H}^+ \rightarrow \text{Na}^+$ . Therefore, to vary the pH, we simply replace one of the protons by  $\text{Na}^+$  and rerun the simulation. This will result in a new polyelectrolyte charge and a new equilibrium pH. Repeating this procedure until all protons inside the cell

have been replaced by sodium ions, we obtain the full titration curve.

## SEMIGRAND CANONICAL REACTIVE MONTE CARLO

We next briefly discuss how the RR-cpH algorithm can be modified to properly account for the requirement of charge neutrality inside the simulation cell. As was stressed previously, the RR-cpH algorithm is intrinsically GC. Therefore, we must treat the system as if it were connected to a reservoir of acid and salt. In a physical system, this would require the presence of a semipermeable membrane, which would allow for a free exchange of ions, but would restrict the motion of polymers to the system’s interior. Since the concentration of counterions is larger inside the system than in the reservoir, they will tend to diffuse into the reservoir, resulting in an electric field and a potential drop across the membrane. This is the physical origin of the Donnan potential,  $\phi_D$ .

The rGCMCD involves the usual GC insertion and deletion moves of individual ions. To preserve the overall charge neutrality inside the cell, a neutralizing background must also be taken into account. The acceptance probabilities for protonation and deprotonation moves are given by<sup>44</sup>

$$\phi_p = 10^{\text{pK}_a - \text{pH}} e^{-\beta(\Delta U_{\text{dc}} + q[\phi_D + \phi_B])}, \\ \phi_d = 10^{\text{pH} - \text{pK}_a} e^{-\beta(\Delta U_{\text{dc}} - q[\phi_D + \phi_B])} \quad (9)$$

Throughout the simulation, the Donnan potential  $\phi_D$  is automatically adjusted to drive the system to a charge-neutral state.<sup>44</sup> The pH in the above equation refers to that of the reservoir, however, knowledge of  $\phi_D$ , also allows us to simultaneously calculate the  $\text{pH}_c$  inside an isolated canonical system using eq 1.<sup>44</sup> We should also note that the presence of a neutralizing background requires a modification of the Bethe potential,  $\phi_B$ .<sup>44</sup> We stress again that the pH of the reservoir is not the same as that of an isolated system of the same ionic content.

We can also combine a protonation move with a GC insertion of an anion into a simulation cell and a deprotonation move with a GC removal of an anion from the cell. The probabilities of such pair moves are, respectively

$$P_p = \min\left[1, \frac{c^{\ominus} V N_A 10^{\text{pK}_a - \text{pH} - \text{pCl}}}{(N_{\text{Cl}} + 1)} e^{-\beta \Delta U}\right] \\ P_d = \min\left[1, \frac{N_{\text{Cl}} 10^{\text{pH} - \text{pK}_a + \text{pCl}}}{c^{\ominus} V N_A} e^{-\beta \Delta U}\right] \quad (10)$$

where  $\text{pCl} = -\log_{10}(a_{\text{Cl}})$ . Note that the Donnan and Bethe potentials cancel out in the pair moves. This algorithm allows us to calculate the protonation state of polyions as a function of pH and salt concentration inside the reservoir. For systems of large volume fractions and low ionic strength, such titration curves will differ significantly from the titration curves of isolated systems of the same polyelectrolyte concentration and salt content.<sup>44</sup> However, if the reservoir contains a large concentration of salt, the Donnan potential will be very small, and the difference between the pH of canonical and GC systems will vanish, see eq 1. This provides us with an additional check of consistency of the different simulation methods presented here. For large ionic strengths, the

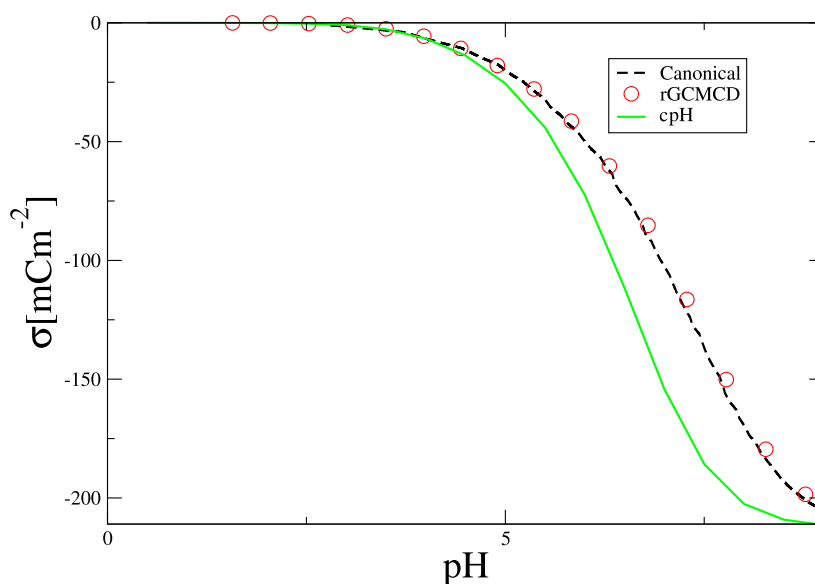


**Figure 1.** Titration curve for a colloidal suspension of 11% volume fraction in the presence of 10 mM salt inside the system. The solid (green) line represents the RR-cpH algorithm, the dashed line represents the canonical simulations, and circles are the results obtained using the rGCMCD algorithm and eq 1 to relate the pH of the reservoir to the pH inside the system.

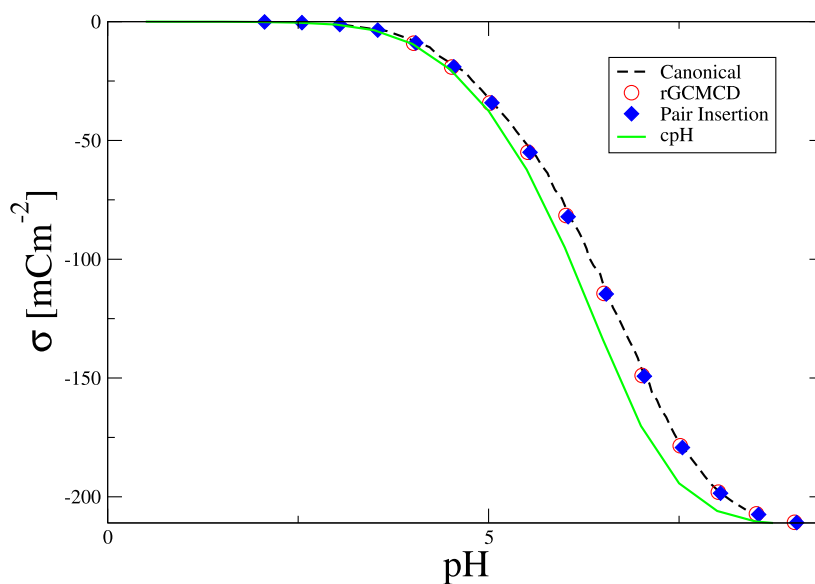


**Figure 2.** Titration curve for a colloidal suspension of 11% volume fraction in the presence of 100 mM salt inside the system. The solid line represents the RR-cpH algorithm, the dashed line represents the canonical simulation, the circles are the results obtained using the rGCMCD and eq 1 to relate the pH of the reservoir to the pH inside the system. Solid (blue) squares are the result of pair-insertion algorithm, eq 10. Note that for large ionic strengths, Donnan potential vanishes, and canonical and grand canonical titration curves become identical.

canonical, rGCMCD, eq 9, and pair insertion algorithms, eq 10, should both produce identical titration curves.

## RESULTS

To compare the predictions of the RR-cpH algorithm with the canonical titration method, we consider a colloidal particle of radius of 60 Å and  $Z = 600$  surface groups. Simulations are carried out within a cubic box of side lengths,  $L$ , containing a colloidal particle at its center. Ewald summation is used to account for Coulomb interactions. In the spirit of the coarse-grained RR-cpH algorithm, we use the primitive model of solvent that treats water as a uniform dielectric continuum of Bjerrum length,  $\lambda_B = q^2/(k_B T \epsilon_w) = 7.2$  Å. Active functional groups have intrinsic  $pK_a = 5.4$ . The simulation cell also

contains the ions  $H_3O^+$ ,  $Cl^-$ , and  $Na^+$ , which we all treat as hard spheres of radius 2 Å with a point charge located at the center.

In Figure 1, we present the titration isotherm of colloidal particles in suspension of volume fraction 11%, containing 10 mM NaCl.

Figure 1 clearly shows that there is a very significant disparity between the results obtained using the RR-cpH algorithm and the canonical-Widom reactive simulation algorithm. Furthermore, the figure also shows that the canonical simulation is in perfect agreement with the results obtained using the rGCMCD method (indicated by the circles), demonstrating the consistency between two very different approaches. We must conclude that for such systems,

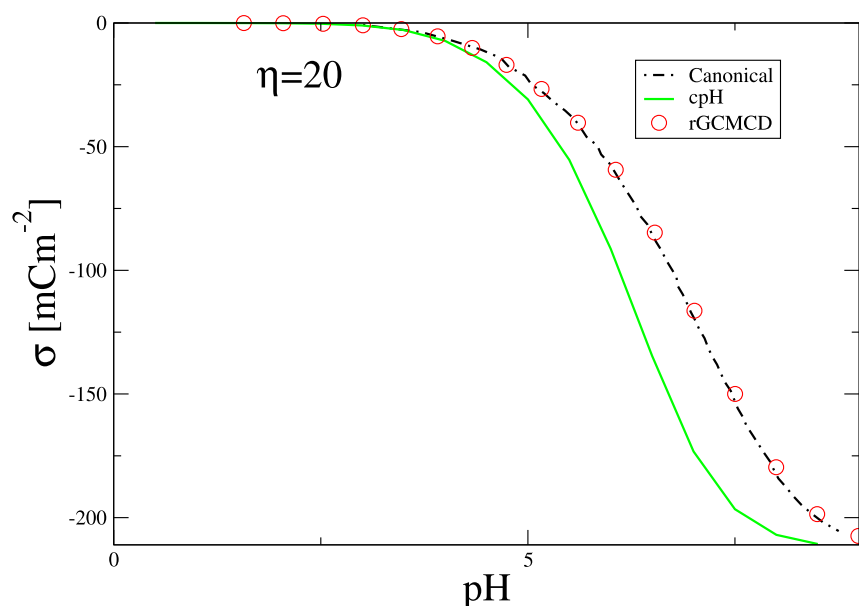


**Figure 3.** Titration curves obtained using the RR-cpH algorithm, canonical titration simulations, and rGCMCD simulation, for colloidal suspension of 20% volume fraction with 10 mM of salt inside the system.

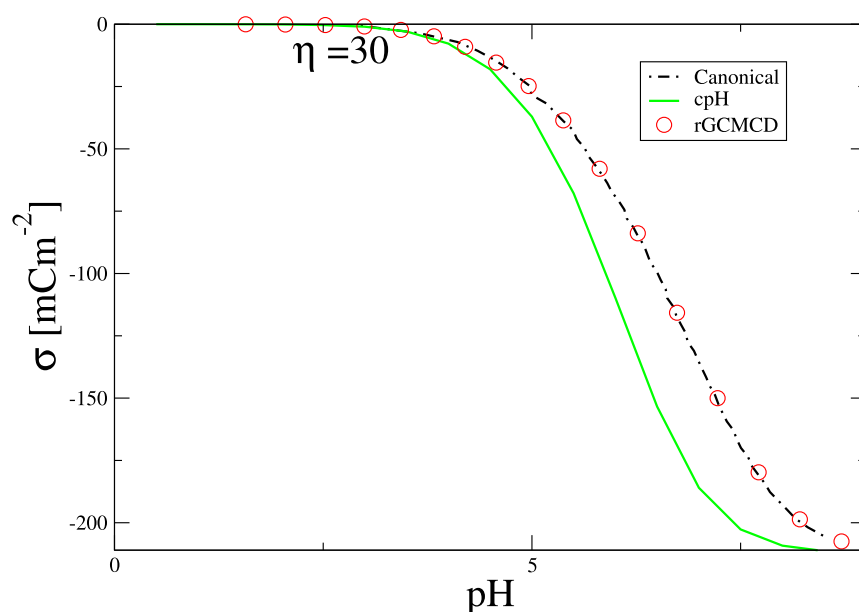


**Figure 4.** Titration curves obtained using the RR-cpH algorithm, canonical titration simulations, and rGCMCD simulation, for colloidal suspension of 30% volume fraction with 10 mM of salt inside the system.

the usual implementation of the RR-cpH algorithm is simply wrong.

For systems containing a large salt concentration, 100 mM, the disparity between the cpH algorithm and canonical simulations diminishes but still remains very significant for intermediate and large pH, as illustrated in Figure 2.

On the other hand, we see a perfect agreement between the canonical, rGCMCD, eq 9, and the pair insertion simulations, eq 10. Recall that for large ionic strengths, the Donnan potential vanishes and the pH of the reservoir is the same as inside the system. Under such conditions, there is no difference between the canonical and GC titration curves.

Finally, we compare the RR-cpH algorithm with canonical titration and rGCMCD simulations for different volume fractions of colloidal particles:  $\eta = 20$  and 30%. Figures 3

and 4 show that the large deviation of RR-cpH algorithm persists for all studied volume fractions, while the rGCMCD and canonical simulation results remain identical.

## CONCLUSIONS


In this paper, we have explored the validity of the usual RR-cpH algorithm. cpH simulations are now a standard tool for investigating charge regulation in coarse-grained models of proteins, polyelectrolytes, and colloidal systems. It is commonly believed that the RR-cpH algorithm can be applied to isolated (canonical) systems. This, however, is not the case. The pH specified in the RR-cpH algorithm refers to that of the reservoir, which because of the presence of the Donnan potential can be very different from that of the system. Furthermore, the arbitrary deletions and insertions of ions,

which are usually performed to preserve the charge neutrality inside the simulation cell, do not respect the detailed balance condition and can lead to very erroneous results.

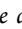
To thoroughly investigate this issue, we conducted a comparative analysis of titration curves generated by the standard RR-cpH algorithm and the exact canonical simulation algorithm. The latter incorporates the recently developed surface Widom insertion method for the pH calculation. Our results reveal a substantial disparity between the titration isotherms obtained through the standard RR-cpH algorithm and the canonical titration algorithm. This underscores the critical importance of employing the correct simulation approach when studying charge regulation in polyelectrolytes, proteins, and colloidal systems.

## AUTHOR INFORMATION

### Corresponding Author

**Yan Levin** – Instituto de Física, Universidade Federal do Rio Grande do Sul, 91501-970 Porto Alegre, Rio Grande do Sul, Brazil;  [orcid.org/0000-0002-0636-7300](https://orcid.org/0000-0002-0636-7300); Email: [levin@if.ufrgs.br](mailto:levin@if.ufrgs.br)

### Author

**Amin Bakhshandeh** – Instituto de Física, Universidade Federal do Rio Grande do Sul, 91501-970 Porto Alegre, Rio Grande do Sul, Brazil;  [orcid.org/0000-0001-5448-5179](https://orcid.org/0000-0001-5448-5179)

Complete contact information is available at:  
<https://pubs.acs.org/10.1021/acs.jctc.3c01360>

### Notes

The authors declare no competing financial interest.

## ACKNOWLEDGMENTS

This work was partially supported by the CNPq, CAPES, and the National Institute of Science and Technology Complex Fluids INCT-FCx.

## REFERENCES

- (1) Bakhshandeh, A.; Frydel, D.; Levin, Y. Theory of Charge Regulation of Colloidal Particles in Electrolyte Solutions. *Langmuir* **2022**, *38*, 13963–13971.
- (2) Frydel, D. General theory of charge regulation within the Poisson-Boltzmann framework: Study of a sticky-charged wall model. *J. Chem. Phys.* **2019**, *150*, 194901.
- (3) Landsgesell, J.; Nová, L.; Rud, O.; Uhlík, F.; Sean, D.; Hebbeker, P.; Holm, C.; Košovan, P. Simulations of ionization equilibria in weak polyelectrolyte solutions and gels. *Soft Matter* **2019**, *15*, 1155–1185.
- (4) Lund, M.; Jönsson, B. On the charge regulation of proteins. *Biochemistry* **2005**, *44*, 5722–5727.
- (5) Jiang, T.; Wang, Z.-G.; Wu, J. Electrostatic Regulation of Genome Packaging in Human Hepatitis B Virus. *Biophys. J.* **2009**, *96*, 3065–3073.
- (6) Prusty, D.; Nap, R.; Szeleifer, I.; Olvera de la Cruz, M. Charge regulation mechanism in end-tethered weak polyampholytes. *Soft Matter* **2020**, *16*, 8832–8847.
- (7) Lund, M.; Åkesson, T.; Jönsson, B. Enhanced protein adsorption due to charge regulation. *Langmuir* **2005**, *21*, 8385–8388.
- (8) Lunkad, R.; da Silva, F. L. B.; Košovan, P. Both Charge-Regulation and Charge-Patch Distribution Can Drive Adsorption on the Wrong Side of the Isoelectric Point. *J. Am. Chem. Soc.* **2022**, *144*, 1813–1825.
- (9) Stornes, M.; Blanco, P. M.; Dias, R. S. Polyelectrolyte-nanoparticle mutual charge regulation and its influence on their complexation. *Colloids Surf., A* **2021**, *628*, 127258.
- (10) Curk, T.; Yuan, J.; Luijten, E. Accelerated simulation method for charge regulation effects. *J. Chem. Phys.* **2022**, *156*, 044122.
- (11) Curk, T.; Luijten, E. Charge Regulation Effects in Nanoparticle Self-Assembly. *Phys. Rev. Lett.* **2021**, *126*, 138003.
- (12) Ong, G. M.; Gallegos, A.; Wu, J. Modeling Surface Charge Regulation of Colloidal Particles in Aqueous Solutions. *Langmuir* **2020**, *36*, 11918–11928.
- (13) Avni, Y.; Andelman, D.; Podgornik, R. Charge regulation with fixed and mobile charged macromolecules. *Fund. Theor. Electrochem. Phys. Nanoelectrochemistry* **2019**, *13*, 70–77.
- (14) Podgornik, R. General theory of charge regulation and surface differential capacitance. *J. Chem. Phys.* **2018**, *149*, 104701.
- (15) Cohen, E. R. *Quantities, Units and Symbols in Physical Chemistry*; Royal Society of Chemistry, 2007.
- (16) Israelachvili, J. N. *Intermolecular and Surface Forces*; Academic Press, 2011.
- (17) Butt, H.-J. A technique for measuring the force between a colloidal particle in water and a bubble. *J. Colloid Interface Sci.* **1994**, *166*, 109–117.
- (18) Levin, Y. Electrostatic correlations: from plasma to biology. *Rep. Prog. Phys.* **2002**, *65*, 1577–1632.
- (19) Andelman, D. Introduction to electrostatics in soft and biological matter. *Soft Condens. Matter Phys. Mol. Cell. Biol.* **2006**, *6*, 97.
- (20) Borkovec, M.; Jönsson, B.; Koper, G. J. M.. In *Surface and Colloid Science*; Matijević, E., Ed.; Springer US: Boston, MA, 2001; pp 99–339.
- (21) Grahame, D. C. The electrical double layer and the theory of electrocapillarity. *Chem. Rev.* **1947**, *41*, 441–501.
- (22) Guldbrand, L.; Jönsson, B.; Wennerström, H.; Linse, P. Electrical double layer forces. A Monte Carlo study. *J. Chem. Phys.* **1984**, *80*, 2221–2228.
- (23) López-García, J.; Aranda-Rascón, M.; Horno, J. Electrical double layer around a spherical colloid particle: The excluded volume effect. *J. Colloid Interface Sci.* **2007**, *316*, 196–201.
- (24) James, R. O.; Parks, G. A. *Surface and Colloid Science*; Springer, 1982; pp 119–216.
- (25) Attard, P. Recent advances in the electric double layer in colloid science. *Curr. Opin. Colloid Interface Sci.* **2001**, *6*, 366–371.
- (26) Carnie, S. L.; Chan, D. Y.; Gunning, J. S. Electrical double layer interaction between dissimilar spherical colloidal particles and between a sphere and a plate: The linearized poisson-boltzmann theory. *Langmuir* **1994**, *10*, 2993–3009.
- (27) Hermansson, M. The DLVO theory in microbial adhesion. *Colloids Surf., B* **1999**, *14*, 105–119.
- (28) Ninham, B. W. On progress in forces since the DLVO theory. *Adv. Colloid Interface Sci.* **1999**, *83*, 1–17.
- (29) Verwey, E. J. W. Theory of the Stability of Lyophobic Colloids. *J. Phys. Colloid Chem.* **1947**, *51*, 631–636.
- (30) Zhou, S. Effective electrostatic interaction between columnar colloids: roles of solvent steric hindrance, polarity, and surface geometric characteristics. *Mol. Phys.* **2023**, *121*, No. e2216632.
- (31) Zhou, S. Effective electrostatic forces between two neutral surfaces with surface charge separation: Valence asymmetry and dielectric constant heterogeneity. *Mol. Phys.* **2022**, *120*, No. e2094296.
- (32) López-Flores, L.; de la Cruz, M. O. Induced phase transformation in ionizable colloidal nanoparticles. *Eur. Phys. J. E* **2023**, *46*, 1–10.
- (33) Zhou, S. Effective electrostatic potential between two oppositely charged cylinder rods in primitive model and extended primitive model electrolytes. *J. Stat. Mech. Theor. Exp.* **2019**, *2019*, 033213.
- (34) Linderstrøm-Lang, K. Om proteinstoffernes ionisation. *Comptes Rendus des Travaux du Laboratoire Carlsberg* **1924**, *15*, 1–29.
- (35) Ninham, B. W.; Parsegian, V. A. Electrostatic potential between surfaces bearing ionizable groups in ionic equilibrium with physiologic saline solution. *J. Theor. Biol.* **1971**, *31*, 405–428.

- (36) Markovich, T.; Andelman, D.; Podgornik, R. Charge regulation: A generalized boundary condition? *Europhys. Lett.* **2016**, *113*, 26004.
- (37) Bakhshandeh, A.; Frydel, D.; Levin, Y. Charge regulation of colloidal particles in aqueous solutions. *Phys. Chem. Chem. Phys.* **2020**, *22*, 24712–24728.
- (38) Bakhshandeh, A.; Frydel, D.; Diehl, A.; Levin, Y. Charge Regulation of Colloidal Particles: Theory and Simulations. *Phys. Rev. Lett.* **2019**, *123*, 208004.
- (39) Bakhshandeh, A.; Segala, M.; Colla, T. E. Equilibrium Conformations and Surface Charge Regulation of Spherical Polymer Brushes in Stretched Regimes. *Macromolecules* **2022**, *55*, 35–48.
- (40) Hosseini, K.; Trus, P.; Frenzel, A.; Werner, C.; Fischer-Friedrich, E. Skin epithelial cells change their mechanics and proliferation upon snail-mediated EMT signalling. *Soft Matter* **2022**, *18*, 2585–2596.
- (41) Reed, C. E.; Reed, W. F. Monte Carlo study of titration of linear polyelectrolytes. *J. Chem. Phys.* **1992**, *96*, 1609–1620.
- (42) Labbez, C.; Jönsson, B. A new Monte Carlo method for the titration of molecules and minerals. *International Workshop on Applied Parallel Computing*; Springer, 2007; Vol. 4699, pp 66–72.
- (43) Levin, Y.; Bakhshandeh, A.; Landsgesell, J.; Nová, L.; Rud, O.; Uhlík, F.; Sean, D.; Hebbeker, P.; Holm, C.; Košovan, P. Simulations of ionization equilibria in weak polyelectrolyte solutions and gels. *Soft Matter* **2019**, *15*, 1155–1185.
- (44) Levin, Y.; Bakhshandeh, A. A new method for reactive constant pH simulations. *J. Chem. Phys.* **2023**, *159*, 111101.
- (45) Ullner, M.; Woodward, C. E. Simulations of the titration of linear polyelectrolytes with explicit simple ions: comparisons with screened Coulomb models and experiments. *Macromolecules* **2000**, *33*, 7144–7156.
- (46) Košovan, P.; Landsgesell, J.; Nová, L.; Uhlík, F.; Beyer, D.; Blanco, P. M.; Staño, R.; Holm, C.; Landsgesell, J.; Nová, L.; Rud, O.; Uhlík, F.; Sean, D.; Hebbeker, P.; Holm, C.; Košovan, P. Simulations of ionization equilibria in weak polyelectrolyte solutions and gels. *Soft Matter* **2019**, *15*, 1155–1185.
- (47) Smith, W.; Triska, B. The reaction ensemble method for the computer simulation of chemical and phase equilibria. I. Theory and basic examples. *J. Chem. Phys.* **1994**, *100*, 3019–3027.
- (48) Johnson, J. K.; Panagiotopoulos, A. Z.; Gubbins, K. E. Reactive canonical Monte Carlo: a new simulation technique for reacting or associating fluids. *Mol. Phys.* **1994**, *81*, 717–733.
- (49) Bakhshandeh, A.; Levin, Y. Canonical titration simulations. *Phys. Chem. Chem. Phys.* **2023**, *25*, 32800–32806.
- (50) Bakhshandeh, A.; Frydel, D.; Levin, Y. Reactive Monte Carlo simulations for charge regulation of colloidal particles. *J. Chem. Phys.* **2022**, *156*, 014108.
- (51) Bakhshandeh, A.; Levin, Y. Titration in Canonical and Grand-Canonical Ensembles. *J. Phys. Chem. B* **2023**, *127*, 9405–9411.
- (52) Landsgesell, J.; Hebbeker, P.; Rud, O.; Lunkad, R.; Košovan, P.; Holm, C. Grand-reaction method for simulations of ionization equilibria coupled to ion partitioning. *Macromolecules* **2020**, *53*, 3007–3020.
- (53) Bakhshandeh, A.; Levin, Y. Widom insertion method in simulations with Ewald summation. *J. Chem. Phys.* **2022**, *156*, 134110.
- (54) Widom, B. Some topics in the theory of fluids. *J. Chem. Phys.* **1963**, *39*, 2808–2812.
- (55) Boda, D.; Giri, J.; Henderson, D.; Eisenberg, B.; Gillespie, D. Analyzing the components of the free-energy landscape in a calcium selective ion channel by Widom's particle insertion method. *J. Chem. Phys.* **2011**, *134*, 02B607.
- (56) Svensson, B. R.; Woodward, C. E. Widom's method for uniform and non-uniform electrolyte solutions. *Mol. Phys.* **1988**, *64*, 247–259.
- (57) Sloth, P.; Sørensen, T. S. Monte Carlo calculations of chemical potentials in ionic fluids by application of Widom's formula: Correction for finite-system effects. *Chem. Phys. Lett.* **1990**, *173*, 51–56.
- (58) de Leeuw, S. W.; Perram, J. W.; Smith, E. R. Simulation of electrostatic systems in periodic boundary conditions. I. Lattice sums and dielectric constants. *Proc. R. Soc. London, A* **1980**, *373*, 27–56.
- (59) Smith, E. R. Electrostatic energy in ionic crystals. *Proc. R. Soc. London, A* **1981**, *375*, 475–505.
- (60) Ballenegger, V. Communication: On the origin of the surface term in the Ewald formula. *J. Chem. Phys.* **2014**, *140*, 161102.
- (61) dos Santos, A. P.; Giroto, M.; Levin, Y. Simulations of Coulomb systems with slab geometry using an efficient 3D Ewald summation method. *J. Chem. Phys.* **2016**, *144*, 144103.
- (62) Euwema, R.; Surratt, G. The absolute positions of calculated energy bands. *J. Phys. Chem. Solids* **1975**, *36*, 67–71.